



12th Canadian Masonry Symposium Vancouver, British Columbia, June 2-5, 2013

PERFORMANCE LIMITS OF BRICK MASONRY SPANDRELS

K. Beyer¹

¹ Assistant Professor, Earthquake Engineering and Structural Dynamics Laboratory (EESD), School of Architecture, Civil and Environmental Engineering (ENAC), Ecole Polytechnique Fédérale de Lausanne (EPFL), Lausanne, Switzerland, katrin.beyer@epfl.ch

ABSTRACT

Spandrel elements in unreinforced brick masonry buildings with timber floors consist of a masonry spandrel supported by either a timber lintel or a masonry arch. When subjected to seismic loading, the force-deformation relationship of such spandrel elements can be described by a piecewise linear relationship which distinguishes two principal regimes: The first regime describes the behaviour up to peak strength of a largely uncracked spandrel. The second regime is associated with a residual strength mechanism after the formation of major cracks in the spandrel. The residual strength of brick masonry spandrels is often less than 80% of their peak strength. Hence, according to established rules in seismic engineering for estimating the ultimate drift capacity of structural members, the residual strength would typically be neglected when assessing the seismic behaviour of existing buildings. However, the residual strength mechanism is typically associated with a rather large deformation capacity and it is therefore argued that it should be considered. Moreover, small cracks due to, for example, previous earthquakes or differential foundation settlements might reduce the peak strength of the spandrel but will have little influence on its residual strength. This paper discusses on the basis of experimental and numerical results the different limit states of brick masonry spandrels subjected to seismic loading, which characterise the two regimes and the ultimate rotation capacity of the spandrel.

KEYWORDS: unreinforced masonry, spandrels, limit states, performance limits, peak strength, residual strength.

INTRODUCTION

Past seismic events have shown that unreinforced masonry (URM) buildings are among the most vulnerable structures during earthquakes. Improved models of their force-deformation behaviour are required to assess their performance during seismic events. Frequently used methods for the seismic analysis of URM buildings are the “equivalent frame approach” (e.g. [1,2]) and the “macro-modelling approach” (e.g. [3-6]). Both modelling approaches require as input the force-deformation characteristics of piers and spandrels (Figure 1a). While such relationships have been proposed for piers, they have yet to be established for spandrels. Recently, based on insights gained from four quasi-static cyclic tests on brick masonry spandrels [7], mechanical models for estimating their peak and residual strength were proposed [8]. To establish piecewise linear force-deformation relationships for spandrels, which can serve as input for equivalent frame models or macro-element models, estimates of the limit rotations are required, which mark the transition from one regime of the spandrel behaviour to another and are linked to different

limit states of the spandrel element. This paper reviews the limit state definitions and their application to masonry piers in Eurocode 8, Part 3 [9], which is one of the few codes proposing limit rotations for piers. It does not, however, provide any guidance to the structural engineer for establishing the force-deformation relationship of masonry spandrels neither regarding their peak and residual strength nor regarding their rotation capacity. The paper connects the definitions of limit states with the corner points of the piecewise linear approximation of the force-deformation relationships of brick masonry spandrels. The spandrel rotation associated with the different limit states are evaluated from quasi-static cyclic tests of four brick masonry spandrels [7] and from results of a numerical study on masonry spandrels, in which spandrel elements were analysed using simplified micro-models [10]. The scope of the paper is limited to solid brick masonry spandrels. To ease the reading, these are in the following referred to as masonry spandrels.

FORCE-DEFORMATION RELATIONSHIPS FOR MASONRY SPANDRELS

A spandrel is a horizontal structural element in a perforated masonry wall. When such a masonry wall is subjected to in-plane horizontal loading, the spandrel is subjected to a deformation mode as shown in Figure 1a and sectional forces as shown in Figure 2a. In a large perforated masonry wall with regular openings and pier dimensions, the spandrel displacement Δ_{sp} and the spandrel rotation θ_{sp} can be computed from (Figure 1b, [11]):

$$\Delta_{sp} = \theta_{pier} (l_{pier} + l_{sp}) \quad (1)$$

$$\theta_{sp} = \theta_{pier} \frac{(l_{pier} + l_{sp})}{l_{sp}} \quad (2)$$

where θ_{pier} is the rotation of the pier, l_{pier} the length of the pier and l_{sp} the length of the spandrel. The geometric relationships between pier and spandrel deformations for a non-regular wall layout can be found in [11]. From the quasi-static cyclic tests on masonry spandrels [7], the envelopes of the cyclic force-deformation relationships were determined and it was found that the envelopes of all four tests can be approximated by the piecewise linear force-rotation relationship shown in Figure 2b [8]. The figure shows on the positive vertical axis the spandrel shear force and on the negative vertical axis the axial compression force in the spandrel as a function of the spandrel rotation θ_{sp} .

The different parts of the piecewise linear force-rotation relationship are associated with different behaviour modes of the spandrel, which were observed during the quasi-static cyclic tests on spandrels [7,8]: For small rotations, the shear force increased almost linearly up to V_{cr} when the first cracks in the spandrel formed (Figure 2b). The stiffness then reduced until the peak shear strength V_p was reached. At this point, the number and size of cracks increased and the spandrel strength dropped to a residual strength V_r which is strongly dependent on the axial force P_{sp} of the spandrel. The onset of material degradation led eventually to a reduced stiffness and strength of the spandrel and finally to its failure. Within the force-rotation relationship of a spandrel, four phases can be distinguished:

- An initial elastic phase up to θ_{p1} ,
- a plateau associated with the peak strength between θ_{p1} and θ_{p2} ,
- the transition between peak and residual strength regime between θ_{p2} and θ_r and
- the residual strength regime between θ_r and θ_{ult} .

The corner rotations θ_{p1} , θ_{p2} , θ_r and θ_{ult} . characterise the transition between the different parts of the force-deformation relationship and can be associated with different damage states [8, 12]. The following sections discuss the limit states defined in Eurocode 8, Part 3 [9] and evaluate the corresponding corner rotations from experimental and numerical results of masonry spandrels.

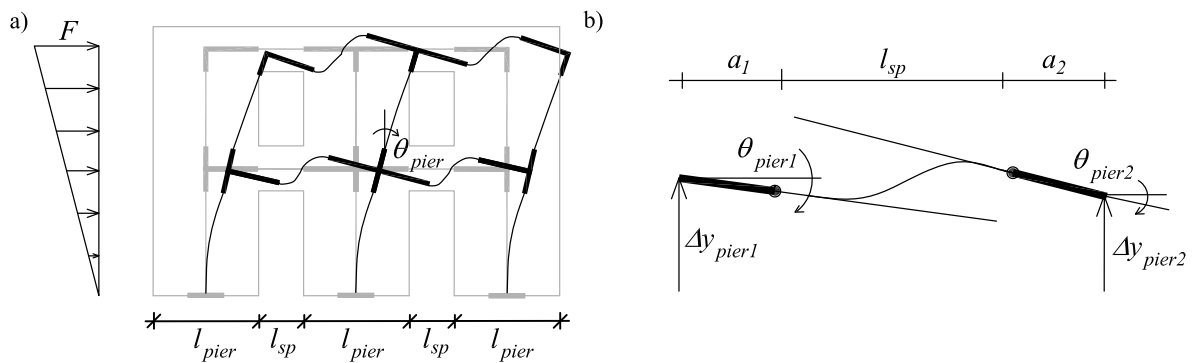


Figure 1 : (a) Deformation of a perforated masonry wall modelled using an equivalent frame model subjected to horizontal in-plane loading. (b) Deformation of the spandrel element in the equivalent frame when the deformations of the pier left and right to the spandrel are equal [8].

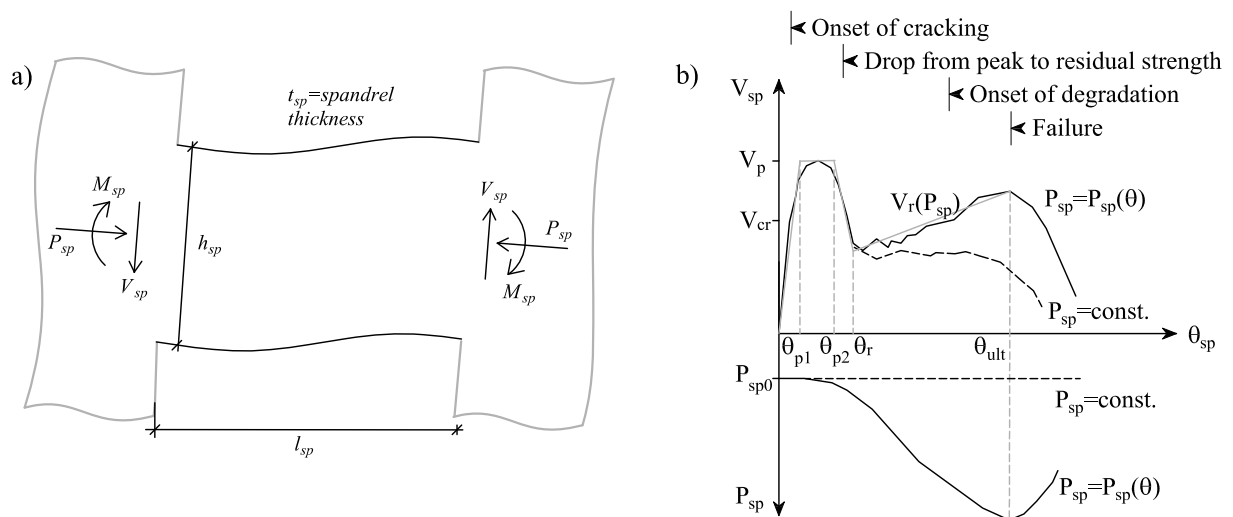


Figure 2 : Deformation of a spandrel subjected to horizontal in-plane loading (a). Characteristic force-deformation relationship of a masonry spandrel subjected to such a deformation (b) [8].

LIMIT STATE DEFINITIONS FOR MASONRY PIERS IN EUROCODE 8, PART 3

Eurocode 8, Part 3 [9] addresses the seismic assessment of existing buildings and provides – unlike its counterpart for new structures Eurocode 8, Part 1 [13] – estimates of drift capacities of URM piers. For URM spandrels, such drift capacities are not defined. This section reviews the drift values and the corresponding limit states definitions in Eurocode 8, Part 3 for unreinforced masonry piers. To ease the reading, Eurocode 8, Part 3 is in the following simply referred to as Eurocode 8.

Eurocode 8 distinguishes between three different limit states, i.e., the limit state “Damage Limitation” (DL), the limit state “Significant Damage” (SD) and the limit state “Near Collapse” (NC). For the limit state “Damage Limitation”, the strength and stiffness of the structure should not be significantly impaired and permanent drifts should be negligible [9]. For a single structural element, this limit state is associated with the yield point of the force-deformation curve, i.e., with the end of the branch corresponding to the elastic response.

The second limit state “Significant Damage” is the limit state on which the seismic assessment of structures is typically based as it describes the limit state which is acceptable for a return period of 475 years of the seismic action. For masonry piers, Eurocode 8 defines drift capacities which are a function of the failure mode and the shear aspect ratio of the pier:

$$\text{Piers failing in shear: } \theta_{SD} = 0.4\% \quad (3)$$

$$\text{Piers failing in flexure: } \theta_{SD} = 0.8\% \frac{H_0}{D} \quad (4)$$

where H_0 is the height of zero moment measured from the base of the pier and D the length of the pier. Eurocode 8 proposes that the drift capacities of piers corresponding to the limit state “Near Collapse” can be obtained by multiplying the drift capacities of the limit state “Significant Damage” by a factor of 4/3. The drift capacities of piers associated with the limit state “Near Collapse” are therefore:

$$\text{Piers failing in shear: } \theta_{NC} = \frac{4}{3} \cdot 0.4\% = 0.53\% \quad (5)$$

$$\text{Piers failing in flexure: } \theta_{NC} = \frac{4}{3} \cdot 0.8\% \frac{H_0}{D} = 1.07\% \frac{H_0}{D} \quad (6)$$

For an entire structure, Eurocode 8 associates the limit state “Near Collapse” with “the roof displacement at which the total lateral resistance (base shear) has dropped below 80% of the peak resistance of the structure, due to progressive damage and failure of lateral load resisting elements.” For single structural members such as a pier or a spandrel, Eurocode 8 does not specify by how much the strength of the element has dropped when the element reaches the limit state “Near Collapse” but describes only qualitatively that the piers might have lost most of their lateral strength and stiffness but should still be able to transfer vertical loads to the foundation. Frumento et al. [14], who set up a harmonised database of pier tests, defined the drift capacity of

piers associated with the limit state “Near Collapse” (θ_{NC}) in the same manner as the drift capacity of an entire structure, i.e., as the drift at which the pier has lost 20% of its peak strength. The limit state rotation “Significant Damage” can then be computed as 75% of the drift θ_{NC} . For the seismic assessment for a return period of 475 years a maximum drift corresponding to the limit state “Significant Damage” should be considered and the bilinear curve is therefore cut off at θ_{SD} .

Eurocode 8 [9] approximates the shear force-drift relationship of masonry piers by a bilinear curve (Figure 3a). In addition to the drift limits noted above, it furnishes estimates of the pier strength. The elastic stiffness of the pier can be computed from gross sectional properties and a stiffness reduction factor of 0.5 to account for cracking. The “yield” drift θ_y , which corresponds to the limit state rotation “Damage Limitation” (θ_{DL}), is the intersection of the elastic branch and the pier strength. Eurocode 8 provides therefore all input required for establishing the shear force-drift relationship of masonry piers. As outlined in the previous section, Eurocode 8 does not provide any guidance for establishing the force-deformation relationship of masonry spandrel or their limit state rotations. The following section aims at transferring the definition of limit state drifts for masonry piers to masonry spandrels.

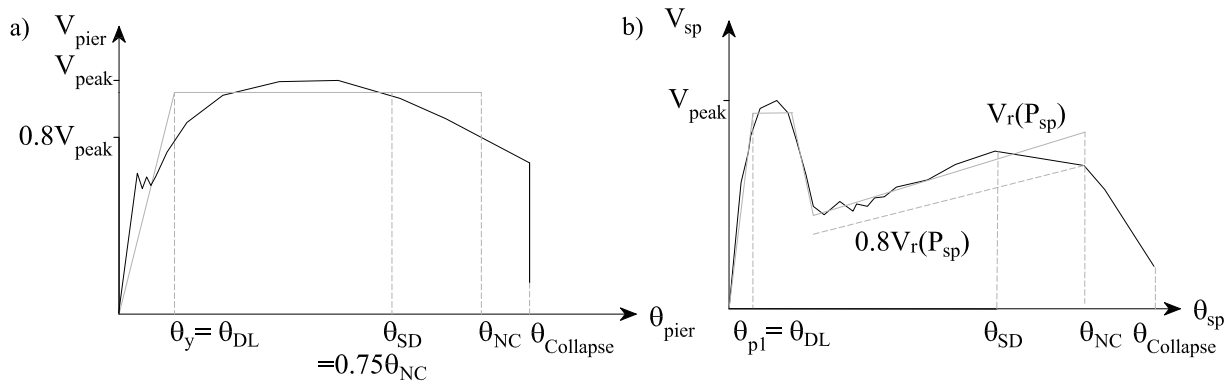


Figure 3 : Limit state rotations according to Eurocode 8: Bilinear force-deformation relationship for masonry piers as defined in Eurocode 8 (a). Piecewise-linear force-deformation relationship of a masonry spandrel and analogues limit state rotations (b).

LIMIT STATES OF MASONRY SPANDRELS

For masonry piers the ultimate rotation capacity, which corresponds to the limit state “Near Collapse”, is defined as the drift at which the strength has dropped below 80% of the pier’s peak strength. If the same definition was applied to spandrels, the ultimate rotation capacity would correspond to a value between θ_{p2} and θ_r and the rather stable force-deformation behaviour of the spandrel for rotations larger than θ_r would be neglected when assessing the seismic performance of the structure. This seems overly conservative and should be avoided.

The description of the limit state “Near Collapse” for an entire structure refers to a very heavily damaged structure with low residual lateral strength and stiffness although the vertical elements are still capable of sustaining vertical loads. As the spandrels are not necessary to transfer the

vertical loads to the foundation, the spandrels could have zero lateral strength and stiffness when the structure attains the limit state “Near Collapse”. The rotation θ_{NC} could therefore be defined as the rotation associated with partial collapse of the spandrel ($\theta_{Collapse}$, Figure 3b), i.e. with the maximum rotation applied during quasi-static cyclic testing. The quasi-static cyclic tests on masonry spandrels showed that the collapse of spandrels supported on timber lintels is caused by the collapse of the lintel supports and that the collapse of spandrels supported on masonry arches starts with the collapse of the arch [7]. However, to be consistent with the definition of the limit rotation θ_{NC} for piers, the limit rotation θ_{NC} of spandrels is defined as the rotation where the residual strength drops by 20% (Figure 3b).

For the limit state “Significant Damage”, Eurocode 8 [9] refers to a structure which is significantly damaged but has still some residual lateral strength and stiffness. The structure can “sustain after-shocks of moderate intensity” but is “likely to be uneconomic to repair”. For masonry spandrels, this definition seems to apply best to the state before the onset of strong material degradation. The onset of degradation can be observed either visually or be determined from the force-rotation relationship of the spandrel as the rotation θ_{SD} before the residual strength deviates from the linear trendline describing the force-rotation relationship of the residual strength regime (Figure 3b).

LIMIT ROTATIONS OBTAINED FROM QUASI-STATIC CYCLIC TESTS ON MASONRY SPANDRELS

The force-deformation envelopes of four masonry spandrels tested under quasi-static cyclic loading [7] were approximated by piecewise linear relationships as the one shown in Figure 3b. The resulting corner points of the piecewise linear envelopes and the limit state rotations are summarised in Table 1. Note that these values are different from the corner points summarised in [12]. The rotations in [12] included the deformations of the adjacent piers. Though small, the pier deformations influence in particular the corner points θ_{p1} , θ_{p2} and θ_r . The ultimate rotation θ_{ult} in [12] corresponds to the limit state “Significant Damage”.

The ratio of the limit state rotation “Near Collapse” and “Significant Damage” is approximately the same for all four test units with a mean ratio of $\theta_{NC}/\theta_{SD}=1.32$ (Table 1). This ratio is very close to the factor of 4/3, which is according to Eurocode 8 the ratio of the drift capacities of piers at the limit states “Near Collapse” and “Significant Damage”. The definition of the limit states for spandrels seems therefore in agreement with the definition of the limit states for piers.

The ratio of the corner rotations that describe the transition from the peak strength regime to the residual strength regime (θ_r/θ_{p2}) is slightly larger than two. The ratio of the corner points that define the length of the plateau of the peak strength regime (θ_{p2}/θ_{p1}) varies significantly between the first two test units TUA/TUB and the third and fourth test unit TUC/TUD. For the latter pair the ratio θ_{p2}/θ_{p1} is approximately twice as large as for the TUA/TUB. TUA and TUB as well as TUC and TUD were constructed pairwise at the same time [7]. TUA and TUB represented masonry spandrels supported on timber lintels while TUC and TUD represented masonry spandrels supported on a shallow masonry arch. The cohesion characterizing the bond between mortar joint and brick was approximately twice as large for TUA/TUB than for TUC/TUD [7].

Numerical analyses on spandrel elements which are presented in the following section showed that the cohesion c and fracture energy G_{fII} of the mortar joints influences the corner rotation θ_{p2} . However, the results of the numerical study show that the effect is considerably less significant than the comparison of TUA/TUB and TUC/TUD might suggest. For this reason, the difference in the corner rotation θ_{p2} might be related to the different configurations of the two pairs of spandrels (i.e. timber lintel vs. masonry arch). For the time being, numerical analyses have only been conducted for masonry spandrels supported on arches. Selected results of these analyses are presented in the following section.

Table 1. Limit state spandrel rotations and corner points of the piecewise linear force-deformation envelopes for TUA-TUD.

Test unit	$\theta_{p1}=\theta_{DL}$ [%]	θ_{p2} [%]	θ_r [%]	θ_{SD} [%]	θ_{NC} [%]	θ_{p2}/θ_{p1}	θ_r/θ_{p2}	θ_{NC}/θ_{SD}
TUA	0.062	0.126	0.27	4.11	5.36	2.04	2.14	1.31
TUB	0.040	0.070	0.15	2.47	3.39	1.77	2.15	1.37
TUC	0.072	0.344	0.82	1.53	2.17	4.77	2.38	1.42
TUD	0.081	0.353	0.810	3.43	4.00	4.37	2.29	1.17
Mean							2.24	1.32
CoV							0.05	0.08

LIMIT ROTATIONS OBTAINED FROM NUMERICAL ANALYSES OF MASONRY SPANDRELS

To determine the limit rotations for more spandrel configurations than those that could be tested experimentally, a simplified micro model of a spandrel element with a masonry arch was set up (Figure 4). Each brick was modelled as a separate unit using plane stress isotropic elements of quadrilateral shape with elastic behaviour. The joints were represented by interface elements with zero thickness. The strength of the interface was described by a Mohr-Coulomb relationship with tension cut-off. The original model represents the test unit TUC [7]. The model was then modified to investigate the effect of the arch geometry, the spandrel geometry, the strength of the joints and the axial load applied to the spandrel on the force-rotation relationship of the spandrel. The models were analysed using the finite element package ATENA [15]. The model validation showed that the numerical model yields reliable estimates of strength and limit rotations for the peak strength regime, i.e., up to the rotation θ_{p2} . For larger rotation, the numerical model tends to overestimate the strength. Details on the model and the model validation can be found in [10].

Figure 5 shows the rotation θ_{p2} as a function of the cohesion c of the interface elements representing the mortar joints and of the mean axial stress p_{sp} on the spandrel. Experimental results and numerical results show different trends for θ_{p2} with c and p_{sp} . In the experimental tests, however, more than one variable was varied at a time. The cohesion was only changed unintentionally as the quality of the mortar differed between TUA/TUB and TUC/TUD. For the test units with the timber lintel (TUA/TUB), the cohesion c was 0.35 MPa while it was only 0.28

MPa for the test units with the masonry spandrel (TUC/TUD). Up to today, numerical analyses have only been conducted for masonry spandrels with arches. To investigate the different trends in experimental and numerical results, numerical analyses should also be conducted for masonry spandrels with timber lintels. For an increase in mean axial stress on the spandrel, the numerically and experimentally determined values of θ_{p2} show a clear positive linear trend. For TUB and TUD, for which the axial force varied during the quasi-static cyclic test, the axial stress p_{sp} was taken as the axial stress p_{sp} at θ_{p2} .

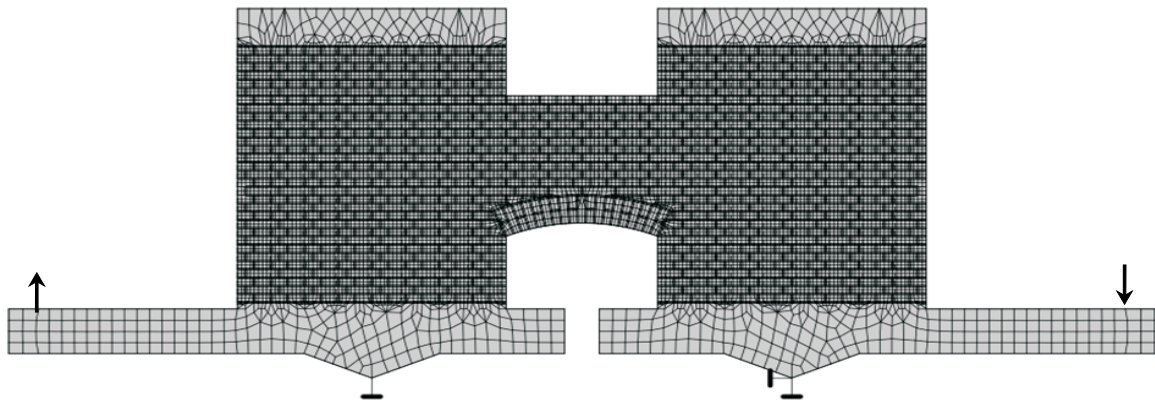


Figure 4 : Numerical model for masonry spandrel with a shallow arch (configuration of TUC) [10].

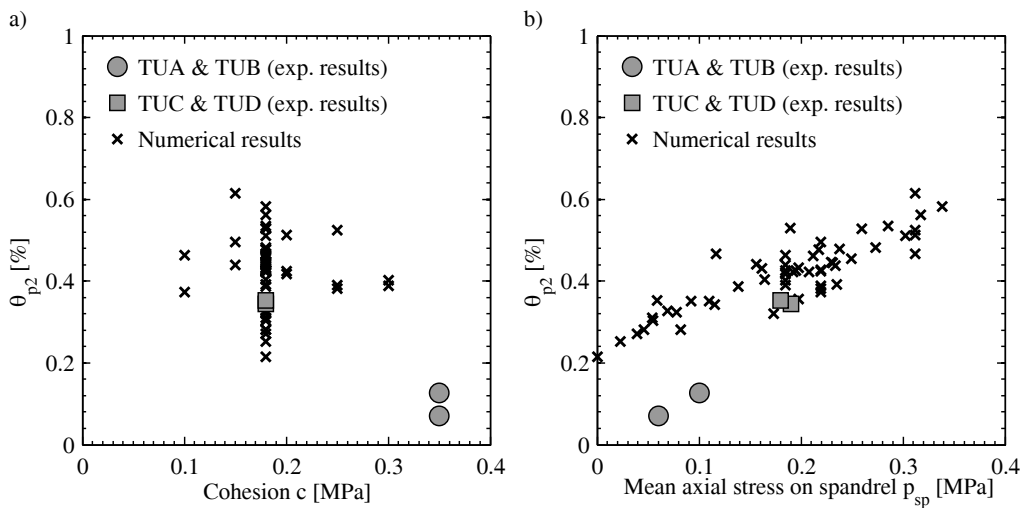


Figure 5 : Limit rotation θ_{p2} as a function of the cohesion c of the mortar joints (a) and of the mean axial stress p_{sp} applied to the spandrel (b).

With respect to the ratio θ_{p2}/θ_{p1} , both numerical and experimental results show a clear decrease of θ_{p2}/θ_{p1} with increasing cohesion c (Figure 6a) while θ_{p2}/θ_{p1} does not seem to be very sensitive to p_{sp} . Hence, the following relationship can be used to estimate the rotation θ_{p2} in function of the rotation θ_{p1} :

$$\theta_{p2} = \theta_{p1} (10 - 25 \cdot c) \quad (7)$$

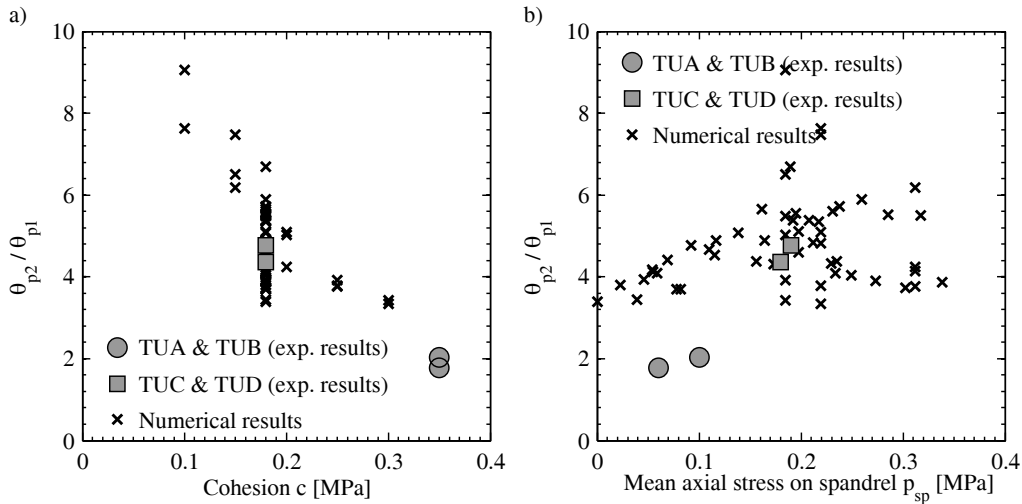


Figure 6 : Limit rotation θ_{p2} as a function of the cohesion c of the mortar joints (a) and of the mean axial stress p_{sp} applied to the spandrel (b).

SUMMARY AND CONCLUSIONS

Masonry spandrels can have a strong influence on the force-deformation relationships of existing masonry structures. For this reason, they should be considered when performing nonlinear pushover analysis using equivalent frame models or macro-element models. Both modelling approaches require as input the force-deformation relationships of piers and spandrels. While such relationships have been proposed for piers, they are yet to be established for spandrels. To predict the force-rotation relationship of a masonry spandrel, estimates of the stiffness, the peak strength, the residual strength and the corner rotations of the piecewise linear relationship are required. Mechanical models for estimating the peak and residual strength have been proposed in [8]. The initial stiffness can be computed from gross sectional properties [10]. The objective of this paper was to propose limit state and corner rotations for masonry spandrels, which would allow predicting the force-rotation relationship of masonry spandrels.

The force-rotation relationship of masonry spandrels can be approximated by a piecewise linear relationship which consists of four parts (Figure 2b): an initial elastic phase up to the “yield” rotation θ_{p1} , a plateau associated with the peak strength between θ_{p1} and θ_{p2} , the transition

between peak and residual strength regime between θ_{p2} and θ_r and the residual strength regime between θ_r and θ_{ult} . The corner rotations can be associated to limit states defined in Eurocode 8, Part 3 [9]. Eurocode 8, Part 3 distinguishes three limit states, i.e., the limit states “Damage Limitation” (DL), “Significant Damage” (SD) and “Near Collapse” (NC). It was proposed that the “yield” rotation θ_{p1} corresponds to the limit rotation θ_{DL} . The ultimate rotation θ_{ult} corresponds to the limit rotation θ_{SD} or θ_{NC} – depending on the return period of the seismic hazard for which the seismic assessment is conducted. The following definitions of the limit state rotations θ_{SD} and θ_{NC} were proposed (Figure 3b):

- The limit state rotation “Significant Damage” should correspond to the rotation before the onset of strong material degradation. This can be observed either visually or – if the axial force P_{sp} of the spandrel is either constant or increases approximately linearly with the spandrel rotation θ_{sp} – from the force-rotation relationship as the rotation before the residual strength deviates from the linear trendline.
- The limit state rotation “Near Collapse” should be taken as the rotation for which the strength has dropped below 80% of the residual strength.

Results from quasi-static cyclic tests on masonry spandrels showed that the mean ratio of the rotations θ_{NC}/θ_{SD} obtained from the results of the spandrel tests is 1.32. This corresponds very well to the drift ratio θ_{NC}/θ_{SD} of 4/3 for piers defined in Eurocode 8. Based on results of experimental and numerical investigations on the force-rotation relationship of masonry spandrels, it is proposed that the corner and limit state rotations of masonry spandrels can be estimated as follows:

- The rotation $\theta_{p1}=\theta_{DL}$ can be estimated as the intersection of the initial stiffness branch with the peak strength V_{peak} [10].
- The ratio θ_{p2}/θ_{p1} decreases as c increases but is not very sensitive to p_{sp} . As a first estimate the rotation θ_{p2} can be estimated from $\theta_{p2} = \theta_{p1} (10 - 25 \cdot c)$.
- The rotation θ_r is approximately twice the rotation θ_{p2} .
- The four tests on masonry spandrels yielded spandrel rotations between 1.5% and 4.1% for the limit state “Significant Damage”.
- The ratio of the limit state rotations θ_{NC}/θ_{SD} is – as for masonry piers – approximately 4/3.

With the definition of the limit state and corner rotations, the force-rotation relationship of masonry spandrels can be estimated. For the rotations θ_r , θ_{SD} and θ_{NC} only experimentally determined values are currently available. For this reason, the estimates are associated with large uncertainties and establishing trends is rather difficult. Future work will therefore aim at refining and validating further the estimates required for describing the residual strength regime of the force-rotation relationship.

ACKNOWLEDGEMENTS

Sujith Mangalathu's contribution to the numerical analyses of the spandrel elements is gratefully acknowledged.

REFERENCES

1. Magenes G, Della Fontana A. (1998) "Simplified non-linear seismic analysis of masonry buildings," Proc. of the British Masonry Society 8: 190-195.
2. Magenes G. (2000) "A method for pushover analysis in seismic assessment of masonry buildings," Proc. of 12th World Conference on Earthquake Engineering, Auckland, New Zealand.
3. Galasco A, Lagomarsino S, Penna A. (2002) "TREMURI Program: Seismic Analyser of 3D Masonry Buildings," Theory and User Manual, University of Genova, Italy.
4. Galasco A, Lagomarsino S, Penna A, Resemini S. (2004) "Non-linear seismic analysis of masonry structures," Proc. of the 13th World Conference on Earthquake Engineering, Vancouver, Canada.
5. Braga F, Liberatore D. (1997) "A finite element for the analysis of the response of masonry buildings," Proc. of the 5th North American Masonry Conference, Urbana, USA.
6. Braga F, Liberatore D, Spera G. (1997) "A computer program for the seismic analysis of complex masonry buildings," Proc. of the 4th International Symposium on Computer Methods in Structural Masonry, Pratolino, Italy.
7. Beyer, K., Dazio, A. (2012) "Quasi-static cyclic tests on masonry spandrels," *Earthquake Spectra* 18(3): 907-929.
8. Beyer, K. (2012) "Peak and residual strengths of brick masonry spandrels," *Engineering Structures* 41: 533-547.
9. CEN (2005) "Eurocode 8: Design of structures for earthquake resistance – Part 3: assessment and retrofitting of buildings," EN 1998-3. European Committee for Standardisation, Brussels, Belgium.
10. Mangalathu, S., Beyer, K., (2012) "Numerical study on the force-deformation behaviour of masonry spandrels with arches," submitted to the *Journal of Earthquake Engineering*.
11. Milani, G., Beyer, K., Dazio, A. (2009) "Upper bound limit analysis of meso-mechanical spandrel models for the pushover analysis of 2D masonry frames," *Engineering Structures*: 31(11), 2696-2710.
12. Beyer, K., Dazio, A. (2012) "Developing force deformation characteristics of brick masonry spandrels in historic buildings," Proc. of the 15th World Conference on Earthquake Engineering, Lisbon, Portugal.
13. CEN (2004) "Eurocode 8: Design of structures for earthquake resistance – Part 1: General rules, seismic actions and rules for buildings," EN 1998-3. European Committee for Standardisation, Brussels, Belgium.
14. Frumento, S., Magenes, G., Morandi, P., Calvi, G.M. (2009) "Interpretation of experimental shear tests on clay brick masonry walls and evaluation of q-factors for seismic design," IUSS Press, Pavia, Italy.
15. Cervenka, V. (2007) "Atena-Computer program for nonlinear finite element analysis of reinforced concrete structures," *Theory and User Manual*, Prague, Czech Republic.